ARTICLE OPEN

Check for updates

Synaptic vulnerability to amyloid-β and tau pathologies differentially disrupts emotional and memory neural circuits

Maria Dolores Capilla-López[1,2], Angel Deprada[1,2], Yuniesky Andrade-Talavera[3], Irene Martínez-Gallego[3], Heriberto Coatl-Cuaya[3], Paula Sotillo[1,2], José Rodríguez-Alvarez[1,2], Antonio Rodríguez-Moreno[3], Arnaldo Parra-Damas[1,2]✉ and Carlos A. Saura[1,2]✉

Alzheimer's disease (AD) is characterized by memory loss and neuropsychiatric symptoms associated with cerebral amyloid-β (Aβ) and tau pathologies, but whether and how these factors differentially disrupt neural circuits remains unclear. Here, we investigated the vulnerability of memory and emotional circuits to Aβ and tau pathologies in mice expressing mutant human amyloid precursor protein (APP), Tau or both APP/Tau in excitatory neurons. APP/Tau mice develop age- and sex-dependent Aβ and phosphorylated tau pathologies, the latter exacerbated at early stages, in vulnerable brain regions. Early memory deficits were associated with hippocampal tau pathology in Tau and APP/Tau mice, whereas anxiety and fear appeared linked to intracellular Aβ in the basolateral amygdala (BLA) of APP and APP/Tau mice. Transcriptome hippocampal profiling revealed gene changes affecting myelination and RNA processing in Tau mice, and inflammation and synaptic-related pathways in APP/Tau mice at 6 months. At 9 months, we detected common and region-specific changes in astrocytic, microglia and 63 AD-associated genes in the hippocampus and BLA of APP/Tau mice. Spatial learning deficits were associated with synaptic tau accumulation and synapse disruption in the hippocampus of Tau and APP/Tau mice, whereas emotional disturbances were linked to Aβ pathology but not synaptic tau in the BLA. Interestingly, Aβ and tau exhibited synergistic detrimental effects in long-term potentiation (LTP) in the hippocampus but they counteract with each other to mitigate LTP impairments in the amygdala. These findings indicate that Aβ and tau pathologies cause region-specific effects and synergize to induce synaptic dysfunction and immune responses, contributing to the differing vulnerability of memory and emotional neural circuits in AD.

Molecular Psychiatry; https://doi.org/10.1038/s41380-025-02901-9

INTRODUCTION

Alzheimer's disease (AD), the major cause of memory loss in the elderly, is accompanied by early neuropsychiatric symptoms that act as early risk factors for conversion to dementia [1, 2]. Cognitive and emotional disturbances are associated with pathological changes in the hippocampus and amygdala at early AD stages [3], but how these brain regions cooperate to cause emotional-related memory changes in AD is unclear. Age and sex affect differentially regional accumulation of amyloid-β (Aβ) and tau pathologies, and cognitive and mood disturbances (depression, anxiety, fear, apathy) [4–7]. In AD mouse models, females with enhanced neuropathology are first affected by anxiety and cognitive deficits [8–14]. Young 3xTg-AD females show higher anxiety and reduced memory retention compared to males [13], whereas sexual dimorphism in behavior, neuropathology and inflammatory molecules are also evident in a tauopathy mouse model [14]. However, how Aβ and tau interact to cause cognitive and neuropsychiatric symptoms remain unclear, in part because emotional factors are largely underrepresented in basic, pathological and clinical studies [15].

Recent evidence in human demonstrates dissociation effects but also a crosstalk of pathological tau- and amyloid-related neural circuit dysconnectivity in memory impairments of AD patients [16–21]. Spatiotemporal pathological changes of tau and Aβ are linked with cognitive decline in aging, and they cause selective regional vulnerability associated with differential gene profiles and cognitive dysfunction in AD [22, 23]. Several studies indicate that Aβ and/or amyloid plaques increase tau phosphorylation, aggregation and seeding [24–28], and tau inactivation ameliorates Aβ-induced memory deficits independently of amyloid pathology [29, 30]. Importantly, Aβ and tau induce synapse dysfunction and loss [31], a pathological feature that tightly correlates with cognitive decline [32–34]. Synaptic tau induces synapse dysfunction, instability and loss [35–38], and it dominates over Aβ on neural circuit disruption [39, 40]. Aβ and tau affect both presynaptic and postsynaptic mechanisms impairing excitatory glutamatergic transmission [35, 41, 42], but whether synaptic tau is responsible and/or synergize with Aβ to induce synapse pathology and behavioral changes is unclear. Moreover, the mechanisms of neuropathological crosstalk between Aβ

[1]Institut de Neurociències, Department de Bioquímica i Biologia Molecular, Facultat de Medicina, Universitat Autònoma de Barcelona, Bellaterra, Barcelona, Spain. [2]Centro de Investigación Biomédica en Red Enfermedades Neurodegenerativas (CIBERNED), Madrid, Spain. [3]Department of Physiology, Anatomy and Cell Biology, Universidad Pablo de Olavide, Sevilla, Spain. ✉email: arnaldo.parra@uab.cat; carlos.saura@uab.cat

Received: 19 April 2024 Revised: 22 December 2024 Accepted: 16 January 2025
Published online: 30 January 2025

and tau leading to synaptic dysfunction and vulnerability of emotional and memory neural circuits are still unknown.

To better elucidate the cellular mechanisms and factors contributing to disruption of cognitive- and emotion-related neural circuits in AD, we generated novel double APP/Tau transgenic mice that recapitulate early synaptic, behavioral, and transcriptional alterations linked to AD pathophysiology. Interestingly, whereas spatial learning and memory deficits were associated with synaptic tau pathology in the hippocampus, emotional disturbances were linked to Aβ in the basolateral amygdala (BLA). Transcriptional profiling revealed hippocampal gene signatures enriched in inflammatory and synaptic pathways affected by early concomitant Aβ/tau pathology but not by Aβ or tau alone. At late stages, specific and coordinated transcriptional responses, including astrocytic, microglia and AD risk genes identified by genome-wide association studies (GWAS) occur in the hippocampus and amygdala of APP/Tau mice. Our study reveals that Aβ and tau affect differentially emotional and memory neural circuits by exerting distinct effects at the transcriptional, functional and behavioral levels.

MATERIALS AND METHODS

Behavioral, biochemical, transcriptomic, immunohistiochemical and electrophysiological methods are extensively described in Supplementary Information.

Mice

Control (WT), APP, Tau and APP/Tau transgenic mice were obtained by crossing heterozygous $APP_{Sw,Ind}$ (line J9; C57BL/6) and Tau P301S (line PS19, JAX #008169; C57BL/6) mice [36, 43], and housed under standard conditions ($n = 4$–6/cage; 22 ± 2 °C, 12 h light:dark cycle). Sex, age and genotypes are indicated in the figure legends. Experimental procedures were approved by the Animal and Human Ethical Committee (CEEAH) of the Universitat Autònoma de Barcelona and local government (CEEAH/DMAH: 2895/10571, 4750/10839) following European Union regulations (2010/63/EU).

Behavioral tests

General and anxiety-like behaviors were studied in the open field and dark/light box (DLB) tests [44, 45] (see Supplementary Information). For cued fear conditioning (CFC), 6 month-old mice were exposed in context A to a conditioned sound stimulus (CS, 2800 Hz, 80 dB; 30 s) followed by an electric footshock (unconditioned stimulus, US, 0.8 mA; 2 s). Freezing behavior was automatically recorded (Video Freeze Software, Med Associates) immediately after the shock (2 min) and again 24 h later in a novel chamber (context B) before (pre-CS; 2 min) and during (CS; 3 min) tone presentation [45]. Mice at 9–10 months were conditioned with two CS-US pairings (context A; US, 1 mA; 2 s). Freezing behavior was recorded during the 2-min interval between pairings and immediately after the shock. At 24 h, 3-min pre-CS period was followed by 16 CS presentations (30 s each, 5-s inter-CS) in context B [46].

Immunohistochemistry

Deparaffinized coronal brain sections (5 µm) were antigen-retrieved with citrate buffer (10 mM, pH 6.0) for tau or with formic acid (60%, 5 min) for Aβ or Aβ/tau, and incubated with anti-phosphorylated (p)tau (Ser202/Thr205, AT8, 1:50; Ser202, CP13, 1:50) or anti-Aβ (6E10, 1:1000) antibodies before biotin-conjugated anti-mouse secondary antibodies (1:200), DAB peroxidase staining (Vector laboratories) and imaging (Nikon Eclipse 80i microscope). For astrocytic and microglial stainings, deparaffined coronal sections (5 µm) were antigen-retrieved (citrate buffer) and incubated with anti-GFAP (Dako Z0334; 1:500) or anti-Iba1 (Wako 019-19741, 1:250) antibodies followed by AlexaFluor-488/594-conjugated goat IgGs (1:400) and Hoechst (1:5000) before imaging (Confocal Zeiss LSM 700 microscope). Immunofluorescence staining with APP/Aβ, anti-Aβ42, pTau and neuronal markers, Iba1 and GFAP quantification [47] and brain atrophy and expansion methods are described in Supplementary Information.

Bulk RNA transcriptional profiling

Bulk RNA-sequencing (RNA-seq) of hippocampus and BLA from 6 and 9 month-old females was performed on an Illumina NextSeq 6000/2000. RNA-seq data analyses, including alignment to the reference genome and differential expression analysis were performed using QuasR/Rhisat2 and DESeq2 packages, and Gene ontology (GO) and functional enrichment analyses using enrichR in Bioconductor [48–50].

Statistical analysis

Statistical analysis was performed using parametric one- or two-way Analysis of Variance (ANOVA) or non-parametric Kruskal-Wallis tests according to D'Agostino-Pearson omnibus normality test (Prism software, GraphPad 8.0.2). For multiple comparisons, we used Sidak's or Tukey's post hocs for parametric tests and Dunn's post hoc for non-parametric test. Parametric unpaired two-tailed Student's t-test or non-parametric Mann-Whitney test, according to D'Agostino-Pearson omnibus normality test, were used when two groups were compared. P values less than 0.05 were considered significant. Adjusted P values (padj) less than 0.1 were considered significant in the transcriptomic analysis. The sample size was calculated using the "Power and Precision" software to ensure adequate power while adhering to the 3Rs principle. Randomization was performed by an independent investigator who assigned animal codes and sample order, ensuring unbiased allocation and blindness to the genotypes during data acquisition. Grubbs' test was used to identify outliers.

RESULTS

Aβ and tau accumulation in excitatory neurons results in age-dependent cerebral AD pathology

To investigate the specific contribution of Aβ and tau on memory and emotional disturbances, we crossed $APP_{Sw,Ind}$ and Tau P301S transgenic mice to generate double APP/Tau transgenic mice that express human *APP* and *Tau* translated transcripts in hippocampal excitatory CaMKIIα but not inhibitory parvalbumin neurons (Supplementary Fig. 1A). Immunofluorescence analysis revealed high localization of hAPP/Aβ (6E10) and total/phosphorylated (p) Tau in excitatory neurons (CaMKIIα, vGlut1, L-glutamate) but not inhibitory interneurons (GAD-67, parvalbumin, somatostatin) in APP/Tau hippocampus, and some colocalization of Aβ with GAD-67 in the BLA (Supplementary Fig. 1B). APP and APP/Tau mice at 6 months show elevated human APP (~2 fold, APP CTF antibody;~17 fold, 6E10), APP α-CTFs and intraneuronal Aβ42 (MOAB-2) but unchanged APP β-CTFs (Supplementary Fig. 2A, B). Tau was similar in Tau and APP/Tau mice (~25 fold) but phosphorylated (p)Tau (Ser202/Thr205) levels were significantly increased in APP/Tau mice (Supplementary Fig. 2A; $P < 0.01$).

APP and APP/Tau mice show similar intracellular Aβ staining in CA1/CA3 hippocampus with no staining in the entorhinal cortex (EC) and BLA at 6 months (Kruskal-Wallis test, CA1: $P < 0.0001$; CA3: $P < 0.0001$; EC: $P > 0.05$; BLA: $P > 0.05$; Fig. 1A). At 9 months, male and female APP and APP/Tau mice show similar number of Aβ-positive neurons and amyloid plaques in hippocampal and cortical regions, except for an increase of Aβ-positive neurons in the EC of females (Two-way ANOVA, EC, genotype effect: $F(3, 37) = 12.78$, $P < 0.0001$; sex effect: $F(1, 37) = 10.10$, $P < 0.01$; interaction: $F(3, 37) = 3.43$, $P < 0.05$; Fig. 1B; Supplementary Fig. 3). The number of pTau (Ser202/Thr205)-positive neurons was significantly increased in APP/Tau mice at 6 months (Kruskal-Wallis test, CA1: $P < 0.001$; CA3: $P < 0.001$; one-way ANOVA, EC: $P < 0.001$; BLA: $P < 0.001$; Fig. 1A). At 9 months, pTau (Ser202, CP13) was prominently increased in neuronal cell bodies and fibers of hippocampus and cortex of male and female Tau and APP/Tau mice (~20–40 fold; Fig. 1B, Supplementary Fig. 3), whereas, compared to males, APP/Tau females show elevated pTau in CA3 (Two-way ANOVA, CA3, genotype effect: $F(3, 35) = 43.57$, $P < 0.0001$; sex effect: $F(1, 35) = 7.87$, $P < 0.01$) (Fig. 1B). Interestingly, APP/Tau mice develop prominent hippocampal atrophy at 9 months ($P < 0.01$–0.0001; Supplementary Fig. 2C). These results demonstrate that APP/Tau mice develop age-dependent Aβ and tau pathologies with no major sex differences.

Hippocampal-dependent learning/memory deficits in young Tau and APP/Tau mice

Analysis of general behavior in the open field revealed no significant differences among genotypes at 6 months in total

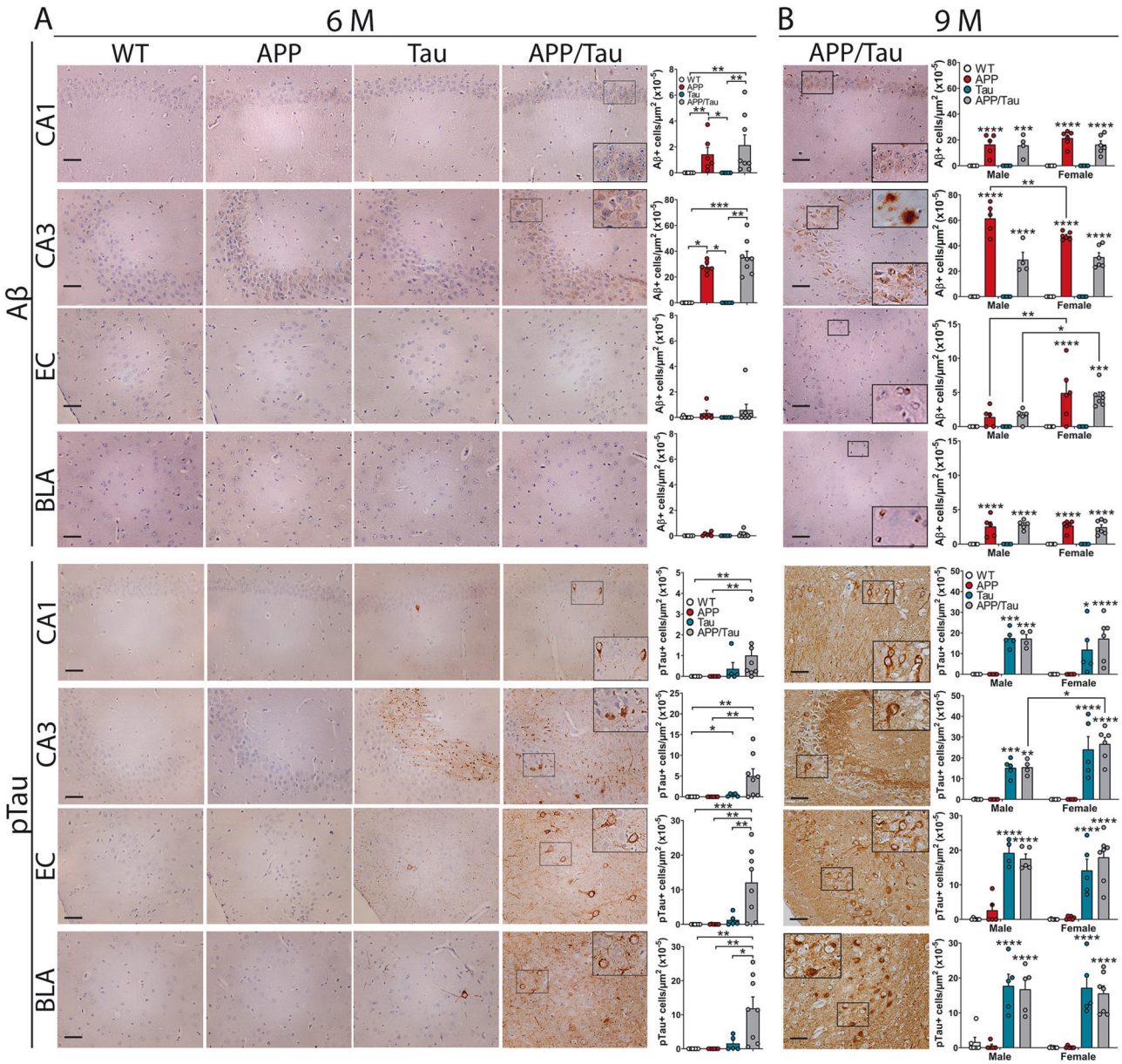

Fig. 1 Aβ potentiates early tau pathology in AD vulnerable brain regions in APP/Tau mice. Coronal brain sections of control (WT), APP, Tau and APP/Tau mice at 6 months (**A**) and 9 months (**B**) were stained with anti-human Aβ/APP (6E10; top) and pTau (Ser202, AT-8 (**A**) or CP13 (**B**); bottom) antibodies. Left images: Representative low and high (insets) magnified images of Aβ- and pTau-stained neurons in CA1 and CA3 hippocampus, entorhinal cortex (EC) and basolateral amygdala (BLA). Amyloid plaques in a 9 month-old APP/Tau mouse are visualized in the top right inset of CA3 region. Objective: 20×. Scale bar: 50 µm. Right diagrams: Quantification of Aβ-positive cells in WT (white symbols), APP (red symbols), Tau (blue symbols), and APP/Tau (grey symbols) mice. Data represent mean number ± SEM of APP/Aβ-and pTau-positive cells/µm^2 ($\times 10^{-5}$) ($n = 3$–4 slices/mouse). Number of mice (male/female), 6 months: WT (2/6), APP (1/5), Tau (0/5) and APP/Tau (3/5); 9 months: WT (6/6), APP (5/6), Tau (5/5) and APP/Tau (4-5/6-7). Statistical analysis was performed using one-way ANOVA or non-parametric Kruskal-Wallis tests according to the D'Agostino-Pearson omnibus normality test, followed by Tukey's or Dunn's post hoc test, respectively (**A**), and two-way ANOVA followed by Sidak's (sex comparison) and Tukey's (genotypes comparison within each sex) multiple comparison tests (**B**). $^{*}P < 0.05$, $^{**}P < 0.01$, $^{***}P < 0.001$, $^{****}P < 0.0001$ *vs* WT or the indicated group.

travelled distance, time inactive and percentage of time in the center (C) and periphery (P) at days 1 and 2 (Supplementary Fig. 4A). DLB and cued fear conditioning (CFC) tests revealed no significant changes in anxiety, neophobia, and fear memory among the transgenic lines at this age (Kruskal-Wallis test and two-way ANOVA, $P > 0.05$; Fig. 2A, B). In the Morris water maze (MWM), all groups showed similar swimming speeds ($P > 0.05$) and decreased latencies during spatial training (Two-way ANOVA, training effect: $F(4, 390) = 37.40$, $P < 0.0001$), although Tau and APP/Tau mice exhibited significantly longer latencies starting at day 2 (Genotype effect: $F(3, 390) = 25.95$, $P < 0.0001$; Fig. 2C, D). In the probe trial, control mice displayed a preference for the target quadrant ($P < 0.05$), whereas APP, Tau and APP/Tau mice showed reduced target quadrant occupancies (Two-way ANOVA, interaction effect: $F(3, 156) = 5.86$, $P < 0.001$) (Fig. 2C, D). This result suggests that spatial learning deficits are associated with hippocampal tau pathology in Tau and APP/Tau mice.

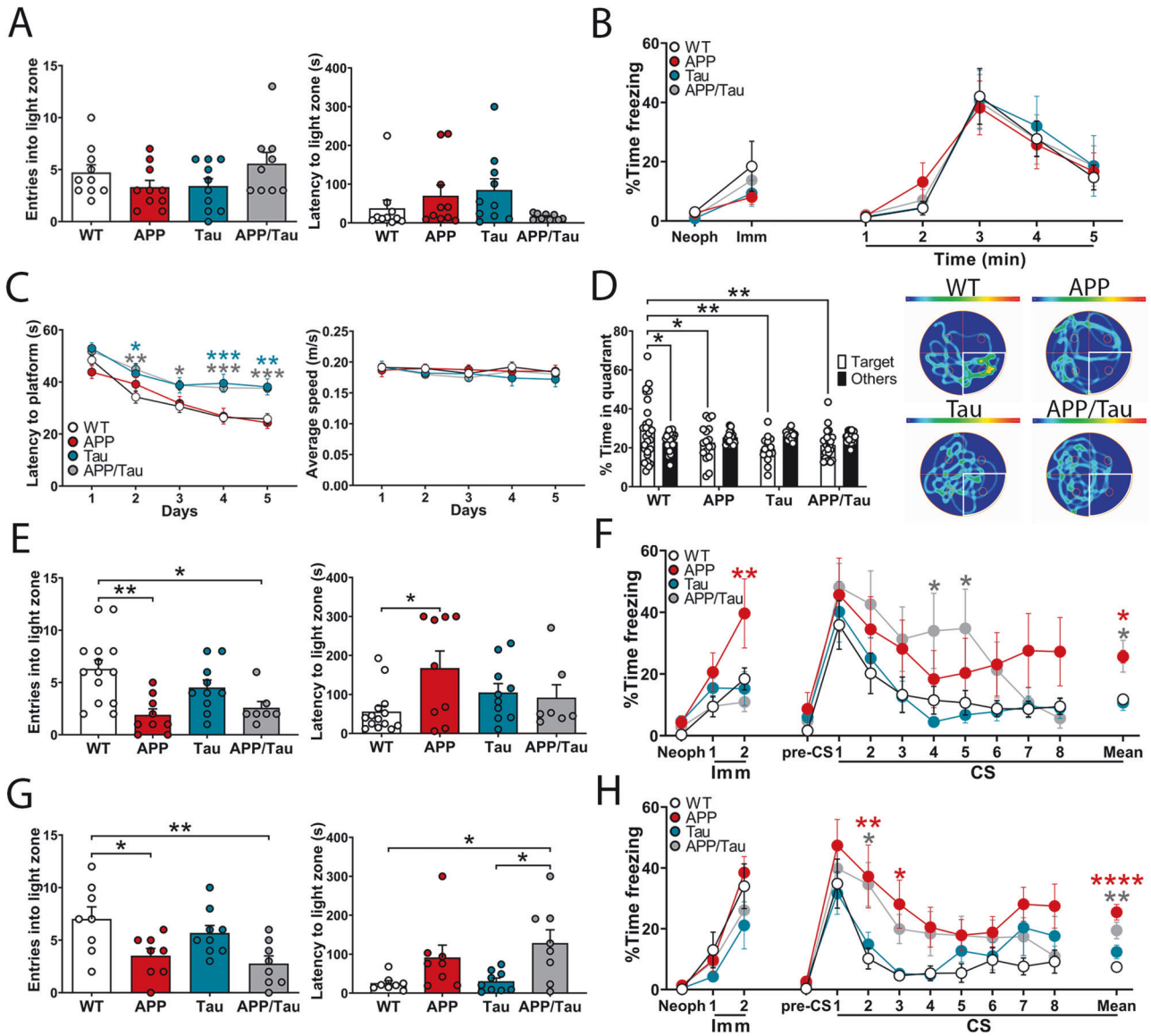

Fig. 2 Differential Aβ and tau effects on spatial memory and emotional disturbances in AD transgenic mice. A–D Behavior of AD transgenic mice at 6 months. **A** Number of entries and latencies to light zone in the DLB test. **B** Associative memory in the fear conditioning test. Freezing responses in the CFC during conditioning (day 1, left) and training (day 2, right) of WT, APP, Tau and APP/Tau mice. **C** Spatial memory training in the MWM for 5 days. **D** % Time in target quadrant *vs* others on day 5 probe trial in the MWM. Heat maps show decreased occupancies and trajectories of transgenic mice in the target quadrant (marked in white). Data represent mean ± SEM. For **A**, **B** number of mice (male/female): WT (4/6), APP (5/5), Tau (2/8) and APP/Tau (4-5/4). For **C**, **D** number of mice (male/female): WT (12/15), APP (11/6), Tau (7/8) and APP/Tau (9/14). **E–H** Behavior of AD transgenic mice at 9 months. **E**, **G** Anxiety behavior of male (**E**) and female (**G**) mice in the dark/light test. **F**, **H** Associative memories of male (**F**) and female (**H**) mice in the CFC test. Freezing responses during conditioning (day 1) and training (CS 1: conditioned stimulus 1) or extinction (CS 2–8) on day 2 in the CFC. The mean ± SEM of time freezing (%) during CS (period from 2 to 8) is represented at the right. In all cases, data represent mean ± SEM. Number of mice (male/female) for **E–H**: WT (14/8, white bars/symbols) APP (9/8, red bars/symbols), Tau (10/9, blue bars/symbols) and APP/Tau (7/8, grey bars/symbols). Statistical analysis was determined by one-way or non-parametric Kruskal-Wallis tests followed by Tukey's or Dunn's post hoc test (**A**, **E**, **G**) or two-way ANOVA (**B–D**, **F**, **H**) followed by Tukey's post hoc test for genotype comparisons. $^{*}P < 0.05$, $^{**}P < 0.01$, $^{***}P < 0.001$, $^{****}P < 0.0001$ *vs* the indicated group or control mice (**C**, **F**, **H**).

Age-dependent emotional disturbances in APP and APP/Tau mice

General behavior evaluated in the open field revealed no significant differences in travelled distances in all male and female groups at 9–10 months, except for increased activity on day 1 in APP/Tau females, indicating similar ambulatory locomotor activities (Supplementary Fig. 4B). In the DLB test, 9 month-old APP and APP/Tau mice of both sexes, but not Tau mice, showed reduced entries (One-way ANOVA, male: $F(3, 36) = 6.88$, $P < 0.001$; females: $F(3, 29) = 5.16$, $P < 0.01$), and higher latencies (except male APP/Tau mice; male: $F(3, 36) = 2.98$, $P < 0.05$; females: $F(329) = 4.47$, $P < 0.05$) into the light compartment (Fig. 2E, G), suggesting increased anxiety in APP and APP/Tau mice. In CFC, innate freezing responses before shock (neophobia) and immediately after shock are similar in female groups (Two-way ANOVA, genotype effect: $P > 0.05$), whereas males show a main significant effect of genotype ($F(3, 108) = 5.23$, $P < 0.01$) and treatment ($F(2, 108) = 15.70$, $P < 0.0001$) (Fig. 2F, H). At 24 h, all groups showed similar and significant CS-induced freezing responses indicating fear memory consolidation. However, there was a significant effect of genotype and tone

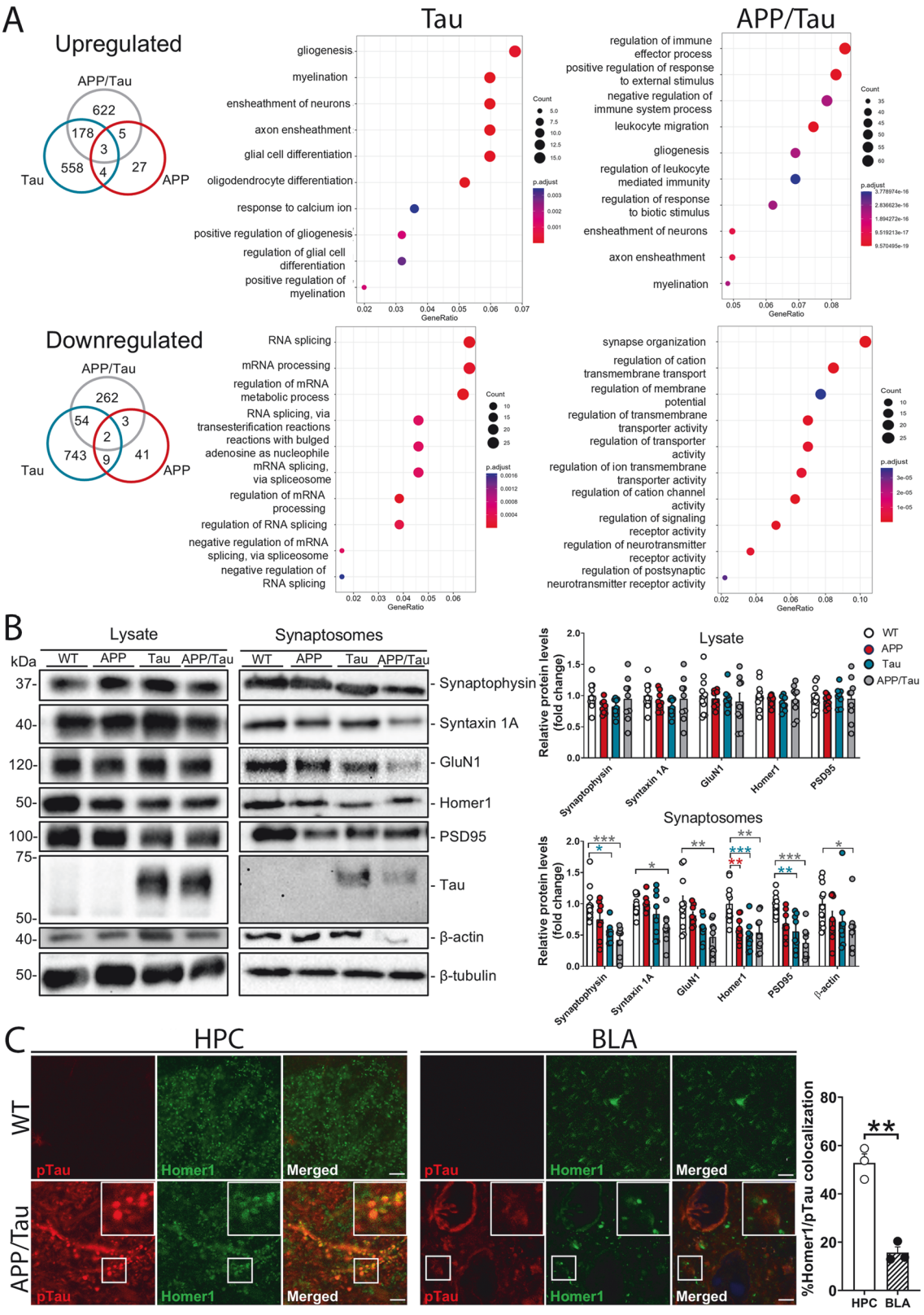

during extinction training (males: genotype effect: $F(3, 324) = 9.57$, $P < 0.0001$; tone effect: $F(8, 324) = 9.51$, $P < 0.0001$; females: genotype effect: $F(3, 306) = 12.56$, $P < 0.0001$; tone effect: $F(8, 306) = 11.48$, $P < 0.0001$) (Fig. 2F, H). Particularly, APP and APP/Tau mice of both sexes show enhanced freezing responses compared to control and Tau mice (One-way ANOVA, male: $F(3, 24) = 7.00$, $P < 0.01$; females: $F(3, 24) = 12.51$, $P < 0.0001$) (Fig. 2F, H). These results indicate that fear-related emotional symptoms are associated with Aβ accumulation in the amygdala of APP and APP/Tau mice.

Fig. 3 Differential transcriptional profiles and synapse pathology in the hippocampus of AD transgenic mice. A Venn and gene ontology diagrams illustrating the differentially expressed genes and enriched cellular pathways altered in the hippocampus of 6 month-old female APP ($n = 8$), Tau ($n = 8$) and APP/Tau mice ($n = 10$) compared with controls (WT, $n = 11$). **B** Biochemical analysis of pre- and post-synaptic proteins and tau (D1M9X antibody) in hippocampal lysates and purified synaptosomes of WT, APP, Tau and/or APP/Tau mice at 6 months ($n = 8$–11 mice/group). Data represent mean levels (fold change) normalized to β-tubulin ± SEM. Number of mice (male/female): 11 WT (6/5, white symbols), 8 APP (5/3, red symbols), 8 Tau (5/3, blue symbols) and 9 APP/Tau (5/4, grey symbols). **C** Confocal microscope images of cleared expanded hippocampal and BLA sections (expansion factor 3.63x) of 6 month-old WT and APP/Tau mice showing colocalization (yellow; quantification at the right graph) of postsynaptic Homer1 (green) and pTau (Ser 202; red) in the CA1 hippocampus but not in the BLA of APP/Tau mice. Right top insets are magnified images of the indicated squared regions. Scale bars: 10 μm and 36.30 μm (expanded). Statistics were determined by one-way ANOVA or Kruskal-Wallis tests followed by Dunnet's or Dunn's multiple comparisons tests according to the normality test, respectively (**B**) or by two-tailed Student's t-test (**C**). $^{*}P < 0.05$, $^{**}P < 0.01$, $^{***}P < 0.001$ *vs* non-transgenic control group.

Early Aβ/tau-induced transcriptional responses in the hippocampus are related to synapse disruption and inflammation

To identify transcriptional responses related to biological pathways affected by early Aβ and tau pathologies, we performed genome-wide bulk RNAseq analysis followed by pathway enrichment analysis in the hippocampus of littermate female WT, APP, Tau and APP/Tau mice at 6 months. Gene expression analysis revealed differentially expressed genes (DEGs) in the hippocampus of APP (94: 39 up, 55 down), Tau (1551: 743 up, 808 down) and APP/Tau (1129: 808 up, 321 down) mice (Fig. 3A). In APP mice, we found significant upregulation of genes related to metabolic processes (*Idh1*, *Ugt2b34*) and oxidative stress (*Prdx1*, *Gstm1*), the latter shared with APP/Tau mice but not Tau mice. GO analysis revealed that the top significantly enriched pathways of the upregulated genes were related to gliogenesis and axon ensheathment/myelination in Tau mice (*Bmp2*, *Dlx2*, *Cst7*, *Itgax, Opalin, Tenm4*), and immune responses in APP/Tau mice (*Aif1*, *C3*, *Cd9*, *Clu, Cnp, Cxcl5, Sox10*). By contrast, downregulated genes were related to RNA processing/splicing in Tau mice (*Cdk9*, *Celf3, Celf5, Mettl3, Srsf7, Ybx2*), and synapse organization, transporters and receptors in APP/Tau mice (*Bdnf*, *Cacnb3*, *Fgf13*, *Dlg4*, *Negr1, Nptxr*). The common upregulated (178) and downregulated (54) genes shared between Tau and APP/Tau mice were related to myelination/glial differentiation and synapse organization/transmission pathways, respectively (not shown). Consistently, cellular pathways related to immune/leukocyte responses (upregulation) and synapse function/ion transporters/neurotransmitter receptors (downregulation) were altered in APP/Tau hippocampus at 6 and 9 months of age (Supplementary Fig. 5A). These results indicate that Aβ and tau cooperate to induce synaptic disruption and immune responses at the transcriptional level.

We next examined pre- and post-synaptic proteins and tau in purified hippocampal synaptosomes and/or brain sections of 6 month-old mice. Biochemical analysis revealed no major changes in synaptic proteins in hippocampal lysates of transgenic mice despite ~45% of APP/Tau mice showed decrease of these proteins (Fig. 3B). In purified hippocampal synaptosomes, we found decrease of Homer-1 in APP mice, and synaptophysin, Homer-1 and PSD95 in Tau mice, whereas all analyzed synaptic proteins and β-actin were decreased in APP/Tau mice (Fig. 3B). Tissue expansion revealed high colocalization of pTau (Ser 202) with the glutamatergic postsynaptic protein Homer1 in the hippocampus (53%) but not in the BLA (15%) of APP/Tau mice (Fig. 3C). Changes in pre- and post-synaptic proteins occur in parallel with synaptic tau accumulation (Fig. 3B), which suggests that synaptic pathological tau contributes to hippocampal synapse pathology in APP/Tau mice.

Tau and Aβ cooperate to induce differential brain regional effects in synaptic plasticity

We next investigated the functional effects of neuronal amyloid and tau pathologies on hippocampal and amygdalar synaptic transmission and plasticity. Input-output curves in Schaffer collateral CA3/CA1 synapses were similarly decreased in all mutant transgenic female mice at 6 months (Two-way ANOVA, stimulus effect: $F(8, 180) = 19.90$, $P < 0.0001$; genotype effect: $F(3, 180) = 34.34$, $P < 0.0001$; interaction effect: $F(24,180) = 2.24$, $P < 0.01$; Fig. 4A). Short-term synaptic plasticity (STP), and long-term potentiation (LTP) induction, measured as early-LTP (60 min) and late-LTP (120 min) were significantly impaired in APP/Tau hippocampus compared with the rest of groups (One-way ANOVA, STP: $F(3, 24) = 4.06$, $P < 0.05$; E-LTP: $F(3, 24) = 3.41$, $P < 0.05$; L-LTP: $F(3, 24) = 7.00$, $P < 0.01$; Fig. 4A–C). Paired-pulse facilitation (PPF) ratio was reduced in APP and APP/Tau mice ($F(3, 21) = 5.37$, $P < 0.01$; Fig. 4D). Whole-cell patch-clamp recordings revealed impaired NMDA responses and NMDA/AMPA ratio in APP/Tau mice ($F(3, 36) = 3.44$, $P < 0.01$; Fig. 4E). These results demonstrate that tau and Aβ cooperate to disrupt hippocampal synaptic plasticity through postsynaptic mechanisms.

In thalamic-LA synapses, basal synaptic transmission was similarly decreased in APP, Tau and APP/Tau mice at 6 months (Two-way ANOVA, stimulus effect: $F(12,481) = 3.45$, $P < 0.0001$; genotype effect: $F(3, 481) = 10.11$, $P < 0.0001$; Fig. 4F). Field recordings revealed decreased STP induction in APP, Tau and APP/Tau mice ($F(3, 34) = 9.01$, $P < 0.001$), and E-LTP and L-LTP deficits in APP and Tau mice but not in APP/Tau mice (E-LTP: $F(3, 34) = 7.61$, $P < 0.001$; L-LTP: $F(3, 34) = 11.29$, $P < 0.0001$; Fig. 4G, H). Basal PPF was reduced in APP mice and recovered in APP/Tau mice ($F(3, 36) = 5.13$, $P < 0.01$; Fig. 4I). NMDA/AMPA ratios were not significantly affected in the transgenic groups ($F(3, 40) = 0.41$, $P > 0.05$; Fig. 4J). Together, these findings indicate that, in contrast to the hippocampus, Aβ and tau counteract each other to maintain synaptic plasticity in the amygdala of young mice.

Coordinated and divergent transcriptional changes related to inflammation and AD-associated genes occur in the hippocampus and BLA of APP/Tau mice

To identify gene signatures and networks differentially affected by late Aβ/tau pathology in the hippocampus and BLA, we next assessed DEGs of female WT and APP/Tau mice at 9 months. We identified 5985 hippocampal genes (3260 up, 2725 down) and 2168 BLA genes (1263 up, 905 down) deregulated in APP/Tau mice, with a high number of DEGs (1423: 24% hippocampus, 65% BLA) coordinately deregulated in both regions (Fig. 5A, B). The most significant enriched pathways affected in both regions were related to neutrophil immune response (upregulation: *Arhgap9, Cd33, Cd68, Itgam, Lamp1, Nfam1, Stk10, Ticam2*) and neurotransmission/glutamate receptor (downregulation: *Camk2a*, *Dlgap1/4, Gria2/3*, *Grin1, Homer1, Lrrk2, Mapk8ip2, Mink1, Shank1, Syn1*) (Fig. 5C). By contrast, the most significantly divergent enriched pathways of upregulated genes in APP/Tau mice were fatty acid metabolism (*Echs1*, *Eci1*, *Echdc3*, *Hadha*, *Hadhb*, *Hsd17b4/10*) in the hippocampus, and Aβ binding, GTPase regulation and oxidoreductase/NAD (*Adrb2*, *Bdh2*, *Hspg2, Itgb2*, *Ncf1/2/4, Rnls*, *Sirt2*, *Sirt5*, *Tlr2*) in the BLA (Fig. 5C; Table 1). In addition, genes highly expressed in reactive astrocytes (*Gfap, ApoE*) and disease-associated microglia (DAM) (*Ccl6*, *Cd33*, *Csf1, Cst7, Cx3cr1*, *Itgax*, *Trem2*, *Tyrobp*) were upregulated in hippocampus and/or BLA of APP/Tau mice (Supplementary Table 1). Accordingly, GFAP and

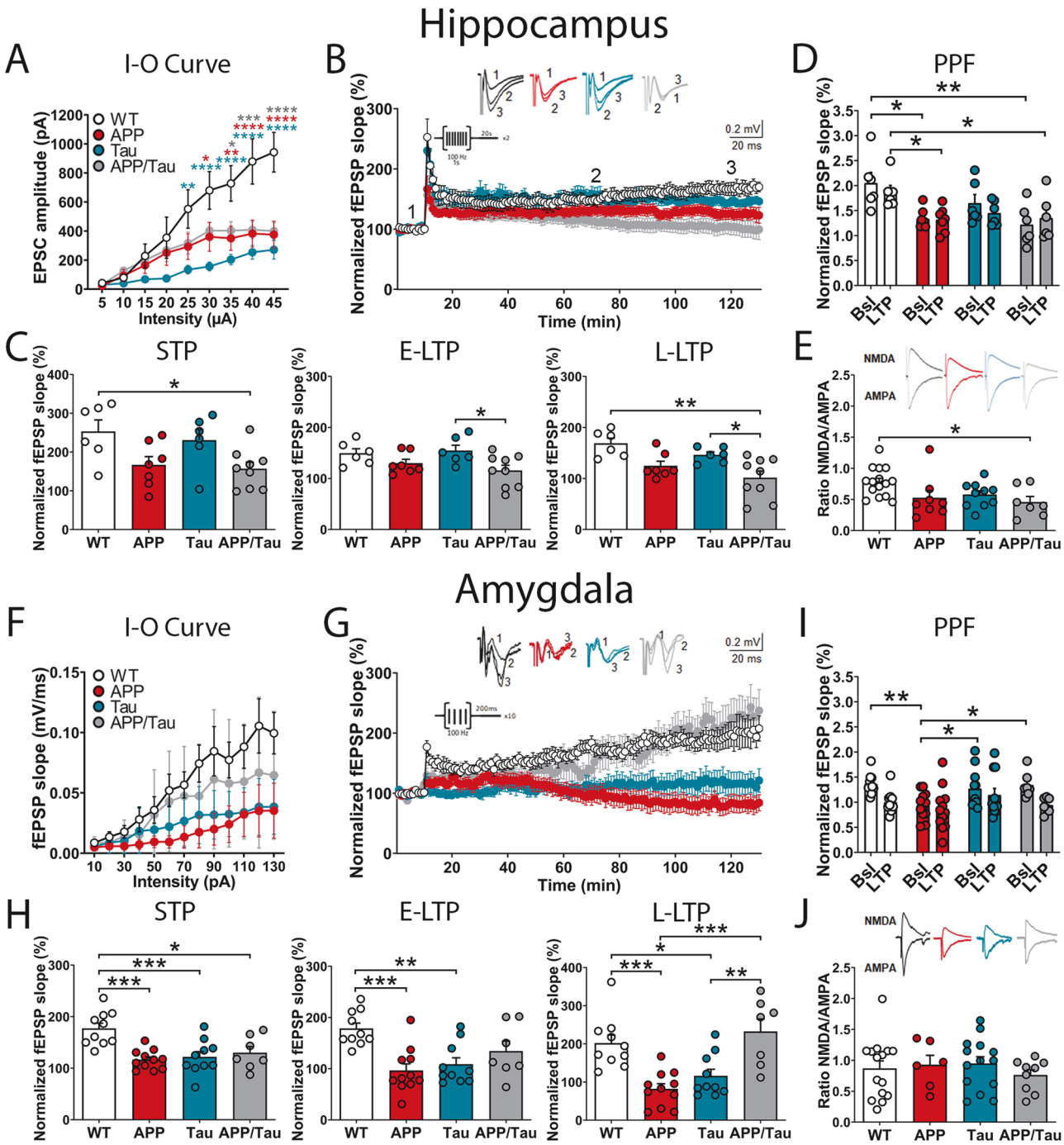

Fig. 4 Brain regional specific effects of tau on Aβ-induced synaptic plasticity impairments. A, F Input-output curves showing EPSC amplitudes (**A**) and fEPSP slope (**F**) *vs* the applied stimulus intensity in CA3/CA1 hippocampal (**A**) and thalamus-lateral amygdala (LA) (**F**) synapses of control (WT, white), APP (red), Tau (blue), and APP/Tau (grey) mice. **B, G** Traces (top) and time course (bottom) of fEPSPs before and after LTP induction in CA3-CA1 hippocampal (**B**) and thalamus-LA synapses (**G**). **C, H** Histograms showing short-term synaptic plasticity (STP), early long-term potentiation (E-LTP), late LTP (L-LTP) in CA3-CA1 hippocampal (**C**) and thalamus-LA synapses (**H**). **D, I** Paired-pulse facilitation (PPF) does not change after LTP induction in the hippocampus (**D**) or amygdala (**I**), and baseline PPFs of APP are decreased in the hippocampus and amygdala compared to controls. However, PPF of APP/Tau mice is significantly decreased only in hippocampus. **E, J** NMDA/AMPA ratio was decreased in hippocampal neurons of APP/Tau mice compared to control, APP, and Tau mice (**E**). In amygdala (**J**), NMDA/AMPA ratio was not affected in the transgenic mice. Data represent mean ± SEM from electrophysiological recordings in CA3-CA1 and thalamic-LA synapses of 6 month-old female control ($n = 7$–8), APP ($n = 5$–6), Tau ($n = 7$–8), and APP/Tau ($n = 6$) mice. Statistical analysis was determined by one-way ANOVA or Kruskal-Wallis tests according to the D'Agostino-Pearson omnibus normality test, followed by Tukey's or Dunn's post hoc test, respectively (**D, E, I, J**) or two-way ANOVA (**A, F**) followed by Tukey's post-hoc test. $^{*}P < 0.05$, $^{**}P < 0.01$, $^{***}P < 0.001$, $^{****}P < 0.0001$ *vs* the indicated group.

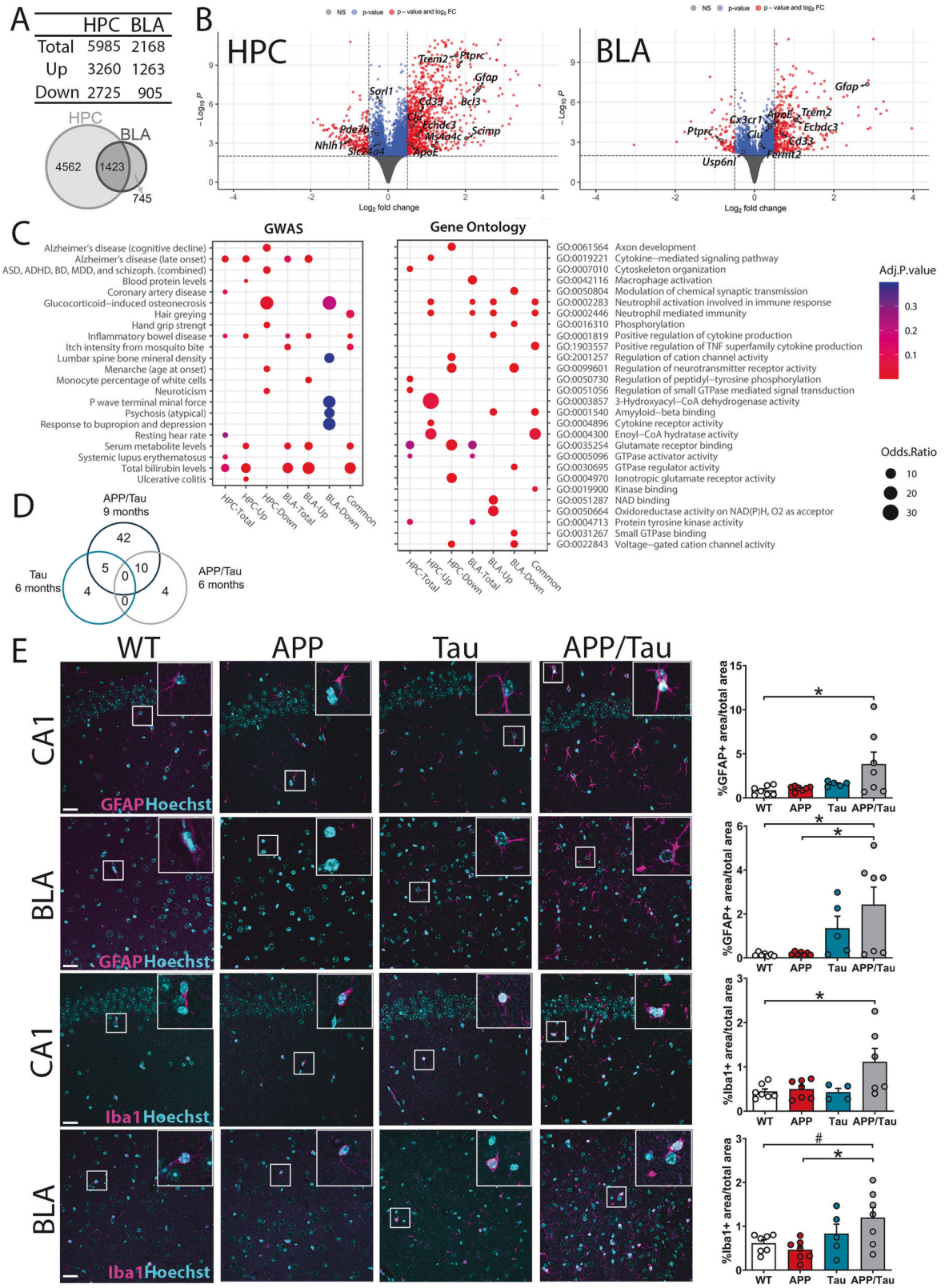

Iba1 stainings were significantly elevated in the CA1/CA3 hippocampus and BLA of APP/Tau mice (One-way ANOVA, $F(3, 22) = 3.51$, $P < 0.05$; BLA: $F(3, 22) = 5.44$, $P < 0.01$; $F(3, 20) = 3.82$, $P < 0.05$; BLA: $F(3, 22) = 4.10$, $P < 0.05$) (Fig. 5E). Importantly, 63 mouse orthologs of human AD-associated genes previously identified in GWAS (e.g, *APOE*, *BIN1*, *CD33*, *CLU*, *MS4A4A*, *PICALM*, *PLCG2*, *PTK2B*, *SLC24A4*, *SORL1*, *TREM2*, *USP6NL*) were deregulated in the hippocampus and/or BLA of female APP/Tau mice (Fig. 5C; Table 1) [51, 52]. Intriguingly, AD-associated genes related to synapse function and ion transport (*NCS1*, *NKAIN2*,

Fig. 5 Bulk RNAseq reveals differential and common gene expression signatures associated with AD in hippocampus and BLA of APP/Tau mice. A Number and Venn diagram illustrating the total, up and down differentially expressed transcripts in the hippocampus (HPC) and BLA of 9 month-old female APP/Tau mice ($n = 9$) compared to controls (WT, $n = 11$ for HPC; $n = 10$ for BLA). **B** Volcano plots showing the fold change of genes differentially expressed in the hippocampus and BLA of APP/Tau mice (cut-off: P value < 0.01, log2FC > 0.5). Some significant deregulated AD risk genes are indicated (see also Table 1). **C** Functional set enrichment of differentially expressed genes in APP/Tau hippocampus and BLA. The plots show the top significantly enriched pathways from the GWAS catalog (2019) (left) and GO Biological Process/ Molecular Function (2021) (right) databases. Human orthologs were used in the analysis with GWAS catalog database. **D** Venn diagram illustrating the AD-associated genes identified previously by GWAS shared in the hippocampus of 6 and 9 month-old female APP/Tau and/or Tau mice. **E** Confocal microscope images (left) and quantification (right graphs) of percentage of GFAP (magenta; top images) and Iba1 (magenta; bottom images) areas, and Hoechst (blue) staining in CA1 hippocampus and BLA sections of female 9 month-old WT ($n = 7$), APP ($n = 7$), Tau ($n = 4–5$) and APP/Tau ($n = 6–7$) mice. Insets are magnified images of the indicated regions. Scale bars: 30 μm. Statistical analysis was determined by one-way ANOVA followed by Tukey's post-hoc test. $^{*}P < 0.05$, $^{\#}P = 0.06$ *vs* the indicated control group.

PDE7B, SLC24A4, SLC4A8, TSPAN13) were specifically downregulated in APP/Tau hippocampus at 9 months. In addition, 23 of these genes were distinctly altered in the hippocampus of APP, Tau and APP/Tau mice at 6 months (Supplementary Fig. 5B). Remarkably, ten mouse orthologs of these human AD-related genes (*AHNAK, ARHGAP20, BCL3, CELF1, CLU, INPP5D, NKAIN2, PDE7B, STK32B, TREM2*) were shared and changed in the same direction in the hippocampus of APP/Tau mice at 6 and 9 months but not in Tau mice (Fig. 5D; Supplementary Table 2). These results suggest that coordinated specific transcriptional responses related to inflammation and synapse function occur in response to Aβ/tau pathology in the hippocampus and BLA.

DISCUSSION

Recent compelling evidence indicates that Aβ and tau pathologies exert synergistic effects on synaptic dysfunction and memory loss, suggesting that therapeutic approaches targeting only one of these factors may not be sufficient for achieving clinical benefits [31, 53]. Accordingly, immunotherapy clinical trials targeting Aβ or tau showed promising biomarker reductions but limited cognitive benefits [54, 55], likely because multiple pathological factors contribute to the disease process [56]. Discerning the pathological mechanisms of Aβ and tau crosstalk is critical to develop effective AD therapies. Importantly, understanding how Aβ and tau pathologies are mechanistically linked in specific brain circuits may help to elucidate their role in cognitive and neuropsychiatric symptoms. Here, we show that APP/Tau mice replicate the key pathological features of AD, including early intracellular Aβ and potentiation of tau pathology, synapse dysfunction, inflammation, neuron loss and deregulation of disease-related gene signatures. Comprehensive analysis of single and double transgenic mice, indicate that Aβ enhances neuronal pathological tau at early disease stages, coinciding with tau-induced disruption of synaptic function, memory, and altered transcriptional profiles related to inflammation and synaptic pathways. Conversely, altered emotional responses were linked to the presence of Aβ in the amygdala at late pathological stages.

Our study reveals distinct pathological vulnerability of memory and emotional circuits, with the presence of pathological tau in hippocampal glutamatergic neurons linked to spatial memory deficits, and Aβ accumulation in the BLA associated with fear emotional disturbances. Hippocampal tau pathology is a strong predictor of memory decline by disconnecting neural networks [18, 57], and synergizes with Aβ to disrupt hippocampal function and memory performance in older adults [16, 17]. The region-specific susceptibility to pathology may be exacerbated by the effect of Aβ on the progression of neuronal tau pathology, as previously shown in double APP-V717I/Tau-P301L mice [58], which can be mediated by cell- or non-cell-autonomous (e.g. microglia) effects [59]. As reported in AD [32, 33, 41, 60], synaptic tau was associated with reduced glutamatergic synaptic proteins and impaired hippocampal-dependent learning in both Tau and APP/Tau mice. This similar phenotype occurs despite significant differences in early hippocampal synaptic plasticity, inflammation, and dysregulation of transcriptional programs, suggesting that alternative cellular and molecular mechanisms converge to induce hippocampal dysfunction in Tau and APP/Tau mice. Based on our transcriptomic analysis, these alternative mechanisms may implicate molecular changes in RNA processing/splicing and synaptic genes/pathways linked to dementia and intellectual disability (e.g. *Bdnf, Cacnb3, Dlg4, Fgf13*…) in Tau and APP/Tau mice, respectively [61–63].

The presence of Aβ pathology in the EC and BLA coincided with anxiety and emotional disturbances in 9–10 month-old APP and APP/Tau mice, further emphasizing the detrimental effects of Aβ on emotional and mood behaviors in AD [45, 64, 65]. Amygdala pathology affects key cellular pathways related to inflammation, neurotransmission, Aβ binding, GTPase activity, and oxidoreductase/NAD+ activity. Given the link among emotional symptoms, inflammation, and neuronal excitability, it is plausible that pharmacological interventions aimed to enhance GABAergic neurotransmission or to mitigate inflammation and oxidative stress could represent promising therapeutic strategies for neuropsychiatric symptoms in dementia [45, 64]. Notably, tau counteracted the Aβ-induced synaptic transmission and plasticity deficits in the amygdala at early stages. The mechanisms underlying tau-mediated protection of synaptic function remain unknown; however, it is intriguing that this coincides with the absence of synaptic tau in this region. As the pathology advances, deficits in this neural circuitry may arise alongside dysregulation of glutamatergic synaptic genes, as observed in APP knock-in mice [66]. Notably, female APP/Tau mice at 9 months exhibited a region-specific increase of Aβ in EC and pTau in CA3 compared to males. This finding is particularly significant considering that women are more susceptible to emotional disturbances and experience faster cognitive decline. The molecular factors driving sex-specific differences in emotional and memory changes remain poorly understood and warrant further investigation. A potential explanation may be the distinct cellular vulnerability of women to pathological changes, including Aβ and/or neurofibrillary tangles [67–70].

The temporal and regional associations of Aβ and tau pathologies with specific behavioral changes do not exclude the possibility that both factors may contribute to memory and emotional decline [17]. Besides the strong correlation between cerebral Aβ deposition and anxiety in elderly non-demented individuals [71, 72], tau and Aβ/tau pathologies are closely associated with neuropsychiatric symptoms in dementia [73, 74]. Considering that anxiety is reversed by anti-tau therapeutic treatments [75–77], the apparent lack of tau effects on emotional symptoms could be explained by dominant effects of Aβ over tau, differences in cell-specific transgene expression and/or age-dependent pathological differences in APP/Tau mice. In this context, gene profiling analysis identified critical genes related to inflammation and synaptic function in two vulnerable brain regions in AD, which is particularly relevant considering the strong correlation between inflammatory and synaptic genes and the progression of AD [78–80]. Nonetheless, our transcriptomic

Table 1. AD-associated genes differentially expressed in the hippocampus and basolateral amygdala of APP/Tau mice.

Biological pathway/gene name	Gene symbol	HPC		BLA		Biological function
		Log_2 FC	padj	Log_2 FC	padj	
Cell adhesion						
CD33 molecule	*CD33*	0.909	0.0002	0.811	0.0112	Carbohydrate and protein binding
Cell adhesion associated, oncogene regulated*	*CDON*	−0.407	0.0129	0.044	0.8796	Protein binding
FERM domain containing kindlin 2**	*FERMT2*	0.072	0.2276	0.160	0.0355	Actin, integrin, and protein kinase binding
Spondin 1	*SPON1*	−0.195	0.0208	−0.468	0.0499	Extracellular matrix structural constituent
Cell differentiation						
Proline rich coiled-coil 2C*	*PRRC2C*	−0.157	0.0357	−0.200	0.2183	RNA binding
Zinc finger CW-type and PWWP domain containing 1*	*ZCWPW1*	0.220	0.0625	−0.085	0.6838	Methylated histone and zinc ion binding
Cell signaling						
CD2 associated protein*	*CD2AP*	0.159	0.0409	0.194	0.2039	Protein binding
GRB2 associated binding protein 2*	*GAB2*	0.251	0.0018	0.077	0.6138	Transmembrane receptor protein tyrosine kinase adaptor activity
Inositol polyphosphate-5-phosphatase D	*INPP5D*	0.911	1.76E-07	0.524	0.0031	Inositol phosphatase activity
IQ motif containing GTPase activating protein 2	*IQGAP2*	−0.337	0.0798	−0.681	0.0159	Actin binding
Myelin protein zero like 1**	*MPZL1*	0.188	0.1824	0.300	0.0347	Structural molecule activity
Ras and Rab interactor 3*	*RIN3*	0.529	0.0098	0.237	0.5371	GTPase activator activity
Rho GTPase activating protein 20*	*ARHGAP20*	−0.338	0.0006	−0.044	0.8427	GTPase activator activity
Serine/threonine kinase 32B*	*STK32B*	−0.412	0.0383	−0.069	0.7908	Protein serine/threonine kinase activity
Cytoskeleton organization						
Bridging integrator 1*	*BIN1*	0.115	0.0115	−0.128	0.4945	Actin filament binding
Cordon-bleu WH2 repeat protein**	*COBL*	−0.002	0.9956	−0.286	0.0663	Actin monomer binding
CUB and Sushi multiple domains 1*	*CSMD1*	−0.315	0.0146	−0.224	0.3286	Protein binding
DLC1 Rho GTPase activating protein**	*DLC1*	−0.018	0.8286	−0.426	0.0880	GTPase activator activity
Electron transport						
Cytochrome c, somatic*	*CYCS*	−0.129	0.0797	−0.108	0.4746	Electron transfer activity
Extracellular matrix organization						
ADAM metallopeptidase with thrombospondin type 1 motif 20**	*ADAMTS20*	−0.040	0.8181	0.344	0.0244	Metalloendopeptidase activity
Thrombospondin type 1 domain containing 4**	*THSD4*	−0.261	0.3363	−0.933	0.0400	Hydrolase activity
Immune response, inflammation						
Clusterin	*CLU*	0.685	0.0015	0.477	0.0059	Aβ and misfolded protein binding
Protein tyrosine kinase 2 beta*	*PTK2B*	−0.274	0.0687	−0.110	0.3080	ATP binding
SLP adaptor and CSK interacting membrane protein*	*SCIMP*	2.519	0.0067	2.527	NA	Molecular adaptor activity
Triggering receptor expressed on myeloid cells 2	*TREM2*	1.849	4.88E-08	1.176	0.0025	Aβ, lipid, and protein binding
Triggering receptor expressed on myeloid cells like 2*	*TREML2*	1.424	7.83E-05	0.389	0.4646	Signaling receptor activity
Lipid metabolism						
Aldehyde oxidase 1	*AOX1*	0.605	5.12E-05	0.616	0.0011	Aldehyde oxidase activity
Apolipoprotein C1	*APOC1*	1.640	0.0002	1.093	0.0461	Lipid binding
Apolipoprotein E	*APOE*	0.744	0.0140	0.556	0.0049	Lipid binding
	ECHDC3	0.914	0.0048	1.207	0.0027	Lyase activity

Table 1. continued

Biological pathway/gene name	Gene symbol	HPC		BLA		Biological function
		Log_2 FC	padj	Log_2 FC	padj	
Enoyl-CoA hydratase domain containing 3						
Phospholipase C gamma 2	*PLCG2*	0.509	0.0124	0.389	0.0982	Phosphatidylinositol and phospholipase activity
Sortilin related receptor 1*	*SORL1*	−0.200	4.69E-05	−0.157	0.1056	Aβ, low-density lipoprotein particle, neuropeptide and GTPase binding
Thromboxane A synthase 1	*TBXAS1*	1.116	0.0010	1.040	3.08E-06	Oxidoreductase activity
UDP glucuronosyltransferase family 1 member A10	*UGT1A10*	1.562	1.19E-08	1.005	0.0001	Glucuronosyltransferase activity
UDP glucuronosyltransferase family 1 member A8	*UGT1A8*	1.569	1.15E-08	0.990	9.72E-05	Glucuronosyltransferase activity
Protein transport and homeostasis						
F-box and leucine-rich repeat protein 7*	*FBXL7*	−0.489	0.0437	0.066	0.8875	Protein binding and ubiquitination
HECT, C2 and WW domain containing E3 ubiquitin protein ligase 1*	*HECW1*	−0.211	0.0285	−0.289	0.1478	Ubiquitin protein ligase activity
Heparan sulfate-glucosamine 3-sulfotransferase 1	*HS3ST1*	0.259	0.0014	0.382	0.0363	Sulfotransferase activity
Rhomboid 5 homolog 1*	*RHBDF1*	0.364	0.0018	0.069	0.7152	Growth factor binding
Sequestosome 1*	*SQSTM1*	0.108	0.0355	−0.024	0.8687	Protein kinase and ubiquitin binding
SEC24 homolog B, COPII coat complex component	*SEC24B*	−0.111	0.0150	−0.120	0.0843	SNARE and zinc ion binding
Transglutaminase 6*	*TGM6*	−1.436	0.0501	−0.852	NA	Protein-glutamine gamma-glutamyltransferase activity
USP6 N-terminal like	*USP6NL*	0.181	0.0521	−0.366	0.0726	GTPase activator activity
Dmx like 1*	*DMXL1*	−0.186	0.0085	−0.087	0.4498	Vacuolar acidification
Synaptic function, ion transport						
Neuronal calcium sensor 1*	*NCS1*	−0.197	0.0298	−0.051	0.4838	Calcium binding
Na+/K+ transporting ATPase interacting 2*	*NKAIN2*	−0.145	0.0029	−0.123	0.2962	Sodium/potassium-transporting ATPase activity
Phosphodiesterase 7B*	*PDE7B*	−0.352	0.0042	0.442	0.4354	c-AMP phosphodiesterase activity
Phosphatidylinositol binding clathrin assembly protein*	*PICALM*	0.104	0.0952	0.022	0.8404	Aβ, SNARE, clathrin, and GTPase binding
Solute carrier family 24 member 4*	*SLC24A4*	−0.257	0.0121	−0.086	0.7272	Calcium/potassium/sodium transporter activity
Solute carrier family 4 member 8*	*SLC4A8*	−0.152	0.0227	−0.132	0.3902	Sodium/bicarbonate/chloride transporter activity
Tetraspanin 13*	*TSPAN13*	−0.211	0.0375	−0.128	0.3426	Calcium channel regulator activity
Transcriptional regulation						
AHNAK nucleoprotein*	*AHNAK*	0.793	0.0072	0.234	0.3389	RNA and protein binding
BCAS3 microtubule associated cell migration factor*	*BCAS3*	−0.122	0.0286	2.299	NA	Acetyltransferase activator activity
BCL3 transcription coactivator*	*BCL3*	2.499	8.48E-06	1.203	0.1014	DNA-binding transcription factor binding
CUGBP Elav-like family member 1*	*CELF1*	−0.134	0.0681	−0.053	0.4822	RNA binding
General transcription factor IIH subunit 3**	*GTF2H3*	−0.089	0.2043	0.198	0.0294	Metal ion binding
Histone deacetylase 9	*HDAC9*	−0.206	0.0724	−0.386	0.0449	DNA-binding transcription factor binding
ST18 C2H2C-type zinc finger transcription factor	*ST18*	−0.229	0.0346	0.389	0.0315	DNA-binding transcription factor activity, RNA polymerase II-specific
Unclassified						
Ataxin 7 like 1*	*ATXN7L1*	−0.141	0.0086	0.022	0.9034	Protein binding
Leucine zipper protein 2	*LUZP2*	−0.187	0.0565	−0.251	0.0840	Extracellular region

Table 1. continued

Biological pathway/gene name	Gene symbol	HPC		BLA		Biological function
		Log_2 FC	padj	Log_2 FC	padj	
Membrane spanning 4-domains A4A	*MS4A4A*	0.705	0.0989	1.178	0.0588	Protein binding
Protein phosphatase 1 regulatory subunit 37*	*PPP1R37*	−0.096	0.0642	−0.040	0.6481	Protein phosphatase inhibitor activity
Transmembrane and coiled-coil domains 4	*TMCO4*	0.708	0.0002	0.467	0.0063	Protein binding

Differential expression of GWAS-identified AD-associated genes in the hippocampus (HPC) and/or basolateral amygdala (BLA) of APP/Tau mice compared with non-transgenic (WT) mice. Genes are grouped according to their biological function sorted alphabetically with Log_2 fold changes (Log_2 FC) indicating downregulated (<0) or upregulated (>0) mRNA levels and significantly deregulated (adjusted *p*-value (padj) <0.1) only in the hippocampus (marked with*) or BLA (marked with**) or in both hippocampus and BLA (not marked).

analysis lacks cell-type resolution, which restricts the identification of the specific cellular population(s) responsible for the transcriptomic alterations underlying the dysfunction of hippocampal and amygdalar neural circuits. By contrast, single-cell transcriptomics showed deregulation of synaptic, signaling, myelination, immune response, metabolism and protein homeostasis pathways in neurons, astrocytes, microglia and oligodendrocytes in AD brain ([81], for a review). In this regard, integrative gene co-expression analyses of murine and human bulk and single-cell transcriptomics may help to identify key cell-type-specific genes affected in specific neural circuits during AD pathology. The deregulation of multiple AD-associated genes related to inflammation, including microglial and astrocytic genes, synapse function and ion transport, suggest their direct relationship with synapse dysfunction and hippocampal-dependent cognitive deficits in AD. Considering that APP/Tau mice exhibit transcriptional changes closely linked to molecular drivers of AD, it may be a useful model for investigating how AD-risk genes contribute to pathological changes and cellular vulnerability in AD.

In summary, our study reveals complex interactions between Aβ and tau, including synergistic and region-specific effects on neuropathology, synapse integrity, immune response, and, ultimately, on cognitive and emotional function. The occurrence of sex-specific differences in pathology, the faithful reproduction of pathological and clinical AD features, and the identification of transcriptional profiles linked to AD risk genes in APP/Tau mice suggest that this may be a useful model for studying sex-specific pathophysiological mechanisms and evaluating novel therapeutic targets. Finally, since both pathologies can alter brain function by affecting different biological processes, we reinforce the need to develop therapeutic approaches in AD that simultaneously target multiple pathophysiological mechanisms.

DATA AVAILABILITY

Raw bulk RNA-seq data were deposited to the Gene Expression Omnibus (GEO) under accession numbers GSE280199 and GSE279050. Data and materials, including specific experimental protocol information, are available under request.

REFERENCES

1. Krell-Roesch J, Syrjanen JA, Vassilaki M, Lowe VJ, Vemuri P, Mielke MM, et al. Brain regional glucose metabolism, neuropsychiatric symptoms, and the risk of incident mild cognitive impairment: the mayo clinic study of aging. Am J Geriatr Psychiatry. 2021;29:179–91.
2. Hwang TJ, Masterman DL, Ortiz F, Fairbanks LA, Cummings JL. Mild cognitive impairment is associated with characteristic neuropsychiatric symptoms. Alzheimer Dis Assoc Disord. 2004;18:17–21.
3. Chaudhary S, Zhornitsky S, Chao HH, van Dyck CH, Li CR. Emotion processing dysfunction in Alzheimer's disease: an overview of behavioral findings, systems neural correlates, and underlying neural biology. Am J Alzheimers Dis Other Demen. 2022;37:15333175221082834.
4. Kim J, Fischer CE, Schweizer TA, Munoz DG. Gender and pathology-specific effect of Apolipoprotein E genotype on psychosis in Alzheimer's disease. Curr Alzheimer Res. 2017;14:834–40.
5. Holland D, Desikan RS, Dale AM, McEvoy LK, Alzheimer's Disease Neuroimaging I. Higher rates of decline for women and apolipoprotein E epsilon4 carriers. AJNR Am J Neuroradiol. 2013;34:2287–93.
6. Hollingworth P, Hamshere ML, Moskvina V, Dowzell K, Moore PJ, Foy C, et al. Four components describe behavioral symptoms in 1120 individuals with late-onset Alzheimer's disease. J Am Geriatr Soc. 2006;54:1348–54.
7. Eikelboom WS, Pan M, Ossenkoppele R, Coesmans M, Gatchel JR, Ismail Z, et al. Sex differences in neuropsychiatric symptoms in Alzheimer's disease dementia: a meta-analysis. Alzheimers Res Ther. 2022;14:48.
8. Hirata-Fukae C, Li HF, Hoe HS, Gray AJ, Minami SS, Hamada K, et al. Females exhibit more extensive amyloid, but not tau, pathology in an Alzheimer transgenic model. Brain Res. 2008;1216:92–103.
9. Melnikova T, Park D, Becker L, Lee D, Cho E, Sayyida N, et al. Sex-related dimorphism in dentate gyrus atrophy and behavioral phenotypes in an inducible tTa:APPsi transgenic model of Alzheimer's disease. Neurobiol Dis. 2016;96:171–85.
10. Schmid S, Rammes G, Blobner M, Kellermann K, Bratke S, Fendl D, et al. Cognitive decline in Tg2576 mice shows sex-specific differences and correlates with cerebral amyloid-β. Behav Brain Res. 2019;359:408–17.
11. Bories C, Guitton MJ, Julien C, Tremblay C, Vandal M, Msaid M, et al. Sex-dependent alterations in social behaviour and cortical synaptic activity coincide at different ages in a model of Alzheimer's disease. PLoS One. 2012;7:e46111.
12. Arsenault D, Tremblay C, Emond V, Calon F. Sex-dependent alterations in the physiology of entorhinal cortex neurons in old heterozygous 3xTg-AD mice. Biol Sex Differ. 2020;11:63.
13. Pairojana T, Phasuk S, Suresh P, Huang SP, Pakaprot N, Chompoopong S, et al. Age and gender differences for the behavioral phenotypes of 3xTg Alzheimer's disease mice. Brain Res. 2021;1762:147437.
14. Sun Y, Guo Y, Feng X, Jia M, Ai N, Dong Y, et al. The behavioural and neuropathologic sexual dimorphism and absence of MIP-3α in tau P301S mouse model of Alzheimer's disease. J Neuroinflammation. 2020;17:72.
15. Ferretti MT, Iulita MF, Cavedo E, Chiesa PA, Schumacher Dimech A, Santuccione Chadha A, et al. Sex differences in Alzheimer disease - the gateway to precision medicine. Nat Rev Neurol. 2018;14:457–69.
16. Düzel E, Ziegler G, Berron D, Maass A, Schutze H, Cardenas-Blanco A, et al. Amyloid pathology but not APOE ε4 status is permissive for tau-related hippocampal dysfunction. Brain. 2022;145:1473–85.
17. Sperling RA, Mormino EC, Schultz AP, Betensky RA, Papp KV, Amariglio RE, et al. The impact of amyloid-β and tau on prospective cognitive decline in older individuals. Ann Neurol. 2019;85:181–93.
18. Harrison TM, Maass A, Adams JN, Du R, Baker SL, Jagust WJ. Tau deposition is associated with functional isolation of the hippocampus in aging. Nat Commun. 2019;10:4900.
19. Pereira JB, Janelidze S, Ossenkoppele R, Kvartsberg H, Brinkmalm A, Mattsson-Carlgren N, et al. Untangling the association of amyloid-β and tau with synaptic and axonal loss in Alzheimer's disease. Brain. 2021;144:310–24.
20. Guo T, Korman D, Baker SL, Landau SM, Jagust WJ, Alzheimer's Disease Neuroimaging I. Longitudinal cognitive and biomarker measurements support a unidirectional pathway in Alzheimer's disease pathophysiology. Biol Psychiatry. 2021;89:786–94.
21. Pascoal TA, Mathotaarachchi S, Mohades S, Benedet AL, Chung CO, Shin M, et al. Amyloid-β and hyperphosphorylated tau synergy drives metabolic decline in preclinical Alzheimer's disease. Mol Psychiatry. 2017;22:306–11.

22. Yu M, Risacher SL, Nho KT, Wen Q, Oblak AL, Unverzagt FW, et al. Spatial transcriptomic patterns underlying amyloid-beta and tau pathology are associated with cognitive dysfunction in Alzheimer's disease. Cell Rep. 2024;43:113691.
23. Kim CM, Diez I, Bueicheku E, Ahn S, Montal V, Sepulcre J. Spatiotemporal correlation between amyloid and tau accumulations underlies cognitive changes in aging. J Neurosci. 2024;44:e0488232023.
24. Grueninger F, Bohrmann B, Czech C, Ballard TM, Frey JR, Weidensteiner C, et al. Phosphorylation of Tau at S422 is enhanced by Aβ in TauPS2APP triple transgenic mice. Neurobiol Dis. 2010;37:294–306.
25. Gotz J, Chen F, van Dorpe J, Nitsch RM. Formation of neurofibrillary tangles in P301l tau transgenic mice induced by Aβ42 fibrils. Science. 2001;293:1491–5.
26. Lewis J, Dickson DW, Lin WL, Chisholm L, Corral A, Jones G, et al. Enhanced neurofibrillary degeneration in transgenic mice expressing mutant tau and APP. Science. 2001;293:1487–91.
27. He Z, Guo JL, McBride JD, Narasimhan S, Kim H, Changolkar L, et al. Amyloid-β plaques enhance Alzheimer's brain tau-seeded pathologies by facilitating neuritic plaque tau aggregation. Nat Med. 2018;24:29–38.
28. Bennett RE, DeVos SL, Dujardin S, Corjuc B, Gor R, Gonzalez J, et al. Enhanced tau aggregation in the presence of amyloid-β. Am J Pathol. 2017;187:1601–12.
29. Roberson ED, Scearce-Levie K, Palop JJ, Yan F, Cheng IH, Wu T, et al. Reducing endogenous tau ameliorates amyloid β-induced deficits in an Alzheimer's disease mouse model. Science. 2007;316:750–4.
30. DeVos SL, Miller RL, Schoch KM, Holmes BB, Kebodeaux CS, Wegener AJ, et al. Tau reduction prevents neuronal loss and reverses pathological tau deposition and seeding in mice with tauopathy. Sci Transl Med. 2017;9:eaag0481.
31. Busche MA, Hyman BT. Synergy between amyloid-β and tau in Alzheimer's disease. Nat Neurosci. 2020;23:1183–93.
32. Pickett EK, Herrmann AG, McQueen J, Abt K, Dando O, Tulloch J, et al. Amyloid-β and tau cooperate to cause reversible behavioral and transcriptional deficits in a model of Alzheimer's sisease. Cell Rep. 2019;29:3592–604.e3595.
33. Ittner LM, Ke YD, Delerue F, Bi M, Gladbach A, van Eersel J, et al. Dendritic function of tau mediates amyloid-β toxicity in Alzheimer's disease mouse models. Cell. 2010;142:387–97.
34. Montero-Crespo M, Dominguez-Alvaro M, Alonso-Nanclares L, DeFelipe J, Blazquez-Llorca L. Three-dimensional analysis of synaptic organization in the hippocampal CA1 field in Alzheimer's disease. Brain. 2021;144:553–73.
35. Hoover BR, Reed MN, Su J, Penrod RD, Kotilinek LA, Grant MK, et al. Tau mislocalization to dendritic spines mediates synaptic dysfunction independently of neurodegeneration. Neuron. 2010;68:1067–81.
36. Yoshiyama Y, Higuchi M, Zhang B, Huang SM, Iwata N, Saido TC, et al. Synapse loss and microglial activation precede tangles in a P301S tauopathy mouse model. Neuron. 2007;53:337–51.
37. Jackson JS, Witton J, Johnson JD, Ahmed Z, Ward M, Randall AD, et al. Altered synapse stability in the early stages of tauopathy. Cell Rep. 2017;18:3063–8.
38. Soto-Faguas CM, Sanchez-Molina P, Saura CA. Loss of presenilin function enhances tau phosphorylation and aggregation in mice. Acta Neuropathol Commun. 2021;9:162.
39. Menkes-Caspi N, Yamin HG, Kellner V, Spires-Jones TL, Cohen D, Stern EA. Pathological tau disrupts ongoing network activity. Neuron. 2015;85:959–66.
40. Busche MA, Wegmann S, Dujardin S, Commins C, Schiantarelli J, Klickstein N, et al. Tau impairs neural circuits, dominating amyloid-β effects, in Alzheimer models in vivo. Nat Neurosci. 2019;22:57–64.
41. Dejanovic B, Huntley MA, De Maziere A, Meilandt WJ, Wu T, Srinivasan K, et al. Changes in the synaptic proteome in tauopathy and rescue of tau-induced synapse loss by C1q antibodies. Neuron. 2018;100:1322–36.e1327.
42. Zhou L, McInnes J, Wierda K, Holt M, Herrmann AG, Jackson RJ, et al. Tau association with synaptic vesicles causes presynaptic dysfunction. Nat Commun. 2017;8:15295.
43. Mucke L, Masliah E, Yu GQ, Mallory M, Rockenstein E, Tatsuno G, et al. High-level neuronal expression of $A\beta_{1-42}$ in wild-type human amyloid protein precursor transgenic mice: synaptotoxicity without plaque formation. J Neurosci. 2000;20:4050–8.
44. Gimenez-Llort L, Garcia Y, Buccieri K, Revilla S, Sunol C, Cristofol R, et al. Gender-specific neuroimmunoendocrine response to treadmill exercise in 3xTg-AD mice. Int J Alzheimers Dis. 2010;2010:128354.
45. España J, Gimenez-Llort L, Valero J, Miñano A, Rabano A, Rodriguez-Alvarez J, et al. Intraneuronal β-amyloid accumulation in the amygdala enhances fear and anxiety in Alzheimer's disease transgenic mice. Biol Psychiatry. 2010;67:513–21.
46. Whittle N, Schmuckermair C, Gunduz Cinar O, Hauschild M, Ferraguti F, Holmes A, et al. Deep brain stimulation, histone deacetylase inhibitors and glutamatergic drugs rescue resistance to fear extinction in a genetic mouse model. Neuropharmacology. 2013;64:414–23.
47. Kang J, Watanabe H, Shen J. Protocols for assessing neurodegenerative phenotypes in Alzheimer's mouse models. STAR Protoc. 2021;2:100654.
48. Gaidatzis D, Lerch A, Hahne F, Stadler MB. QuasR: quantification and annotation of short reads in R. Bioinformatics. 2015;31:1130–2.
49. Love MI, Huber W, Anders S. Moderated estimation of fold change and dispersion for RNA-seq data with DESeq2. Genome Biol. 2014;15:550.
50. Kuleshov MV, Jones MR, Rouillard AD, Fernandez NF, Duan Q, Wang Z, et al. Enrichr: a comprehensive gene set enrichment analysis web server 2016 update. Nucleic Acids Res. 2016;44:W90–97.
51. Wightman DP, Jansen IE, Savage JE, Shadrin AA, Bahrami S, Holland D, et al. A genome-wide association study with 1,126,563 individuals identifies new risk loci for Alzheimer's disease. Nat Genet. 2021;53:1276–82.
52. Bellenguez C, Kucukali F, Jansen IE, Kleineidam L, Moreno-Grau S, Amin N, et al. New insights into the genetic etiology of Alzheimer's disease and related dementias. Nat Genet. 2022;54:412–36.
53. Boxer AL, Sperling R. Accelerating Alzheimer's therapeutic development: the past and future of clinical trials. Cell. 2023;186:4757–72.
54. van Dyck CH, Swanson CJ, Aisen P, Bateman RJ, Chen C, Gee M, et al. Lecanemab in early Alzheimer's disease. N Engl J Med. 2023;388:9–21.
55. Monteiro C, Toth B, Brunstein F, Bobbala A, Datta S, Ceniceros R, et al. Randomized phase II study of the safety and efficacy of semorinemab in participants with mild-to-moderate Alzheimer disease: Lauriet. Neurology. 2023;101:e1391–401.
56. Wilson DM, 3rd, Cookson MR, Van Den Bosch L, Zetterberg H, Holtzman DM, et al. Hallmarks of neurodegenerative diseases. Cell. 2023;186:693–714.
57. Chen X, Cassady KE, Adams JN, Harrison TM, Baker SL, Jagust WJ. Regional tau effects on prospective cognitive change in cognitively normal older adults. J Neurosci. 2021;41:366–75.
58. Terwel D, Muyllaert D, Dewachter I, Borghgraef P, Croes S, Devijver H, et al. Amyloid activates GSK-3β to aggravate neuronal tauopathy in bigenic mice. Am J Pathol. 2008;172:786–98.
59. Green GS, Fujita M, Yang HS, Taga M, Cain A, McCabe C, et al. Cellular communities reveal trajectories of brain ageing and Alzheimer's disease. Nature. 2024;633:634–45.
60. Colom-Cadena M, Davies C, Sirisi S, Lee JE, Simzer EM, Tzioras M, et al. Synaptic oligomeric tau in Alzheimer's disease - A potential culprit in the spread of tau pathology through the brain. Neuron. 2023;111:2170–83.e2176.
61. Ni H, Xu M, Zhan GL, Fan Y, Zhou H, Jiang HY, et al. The GWAS risk genes for depression may be actively involved in Alzheimer's disease. J Alzheimers Dis. 2018;64:1149–61.
62. Shen KF, Yue J, Wu ZF, Wu KF, Zhu G, Yang XL, et al. Fibroblast growth factor 13 is involved in the pathogenesis of temporal lobe epilepsy. Cereb Cortex. 2022;32:5259–72.
63. Kjaer C, Palasca O, Barzaghi G, Bak LK, Durhuus RKJ, Jakobsen E, et al. Differential expression of the β3 subunit of voltage-gated Ca2+ channel in mesial temporal lobe epilepsy. Mol Neurobiol. 2023;60:5755–69.
64. Van der Jeugd A, Parra-Damas A, Baeta-Corral R, Soto-Faguas CM, Ahmed T, LaFerla FM, et al. Reversal of memory and neuropsychiatric symptoms and reduced tau pathology by selenium in 3xTg-AD mice. Sci Rep. 2018;8:6431.
65. Johansson M, Stomrud E, Johansson PM, Svenningsson A, Palmqvist S, Janelidze S, et al. Development of apathy, anxiety, and depression in cognitively unimpaired older adults: Effects of Alzheimer's disease pathology and cognitive decline. Biol Psychiatry. 2022;92:34–43.
66. Arroyo-Garcia LE, Isla AG, Andrade-Talavera Y, Balleza-Tapia H, Loera-Valencia R, Alvarez-Jimenez L, et al. Impaired spike-gamma coupling of area CA3 fast-spiking interneurons as the earliest functional impairment in the App(NL-G-F) mouse model of Alzheimer's disease. Mol Psychiatry. 2021;26:5557–67.
67. Wolfova K, Creese B, Aarsland D, Ismail Z, Corbett A, Ballard C, et al. Gender/sex differences in the association of mild behavioral impairment with cognitive aging. J Alzheimers Dis. 2022;88:345–55.
68. Buckley RF, Scott MR, Jacobs HIL, Schultz AP, Properzi MJ, Amariglio RE, et al. Sex mediates relationships between regional tau pathology and cognitive decline. Ann Neurol. 2020;88:921–32.
69. Lin KA, Choudhury KR, Rathakrishnan BG, Marks DM, Petrella JR, Doraiswamy PM, et al. Marked gender differences in progression of mild cognitive impairment over 8 years. Alzheimers Dement (N Y). 2015;1:103–10.
70. Barnes LL, Wilson RS, Bienias JL, Schneider JA, Evans DA, Bennett DA. Sex differences in the clinical manifestations of Alzheimer disease pathology. Arch Gen Psychiatry. 2005;62:685–91.
71. Johansson M, Stomrud E, Lindberg O, Westman E, Johansson PM, van Westen D, et al. Apathy and anxiety are early markers of Alzheimer's disease. Neurobiol Aging. 2020;85:74–82.
72. Cai WJ, Tian Y, Ma YH, Dong Q, Tan L, Yu JT, et al. Associations of anxiety with amyloid, tau, and neurodegeneration in older adults without dementia: a longitudinal study. J Alzheimers Dis. 2021;82:273–83.
73. Tissot C, Therriault J, Pascoal TA, Chamoun M, Lussier FZ, Savard M, et al. Association between regional tau pathology and neuropsychiatric symptoms in aging and dementia due to Alzheimer's disease. Alzheimers Dement. 2021;7:e12154.

74. Therriault J, Pascoal TA, Savard M, Benedet AL, Chamoun M, Tissot C, et al. Topographic distribution of amyloid-β, tau, and atrophy in patients with behavioral/dysexecutive Alzheimer disease. Neurology. 2021;96:e81–92.
75. Nisbet RM, Van der Jeugd A, Leinenga G, Evans HT, Janowicz PW, Gotz J. Combined effects of scanning ultrasound and a tau-specific single chain antibody in a tau transgenic mouse model. Brain. 2017;140:1220–30.
76. Anglada-Huguet M, Rodrigues S, Hochgrafe K, Mandelkow E, Mandelkow EM. Inhibition of Tau aggregation with BSc3094 reduces Tau and decreases cognitive deficits in rTg4510 mice. Alzheimers Dement (N Y). 2021;7:e12170.
77. Di J, Siddique I, Li Z, Malki G, Hornung S, Dutta S, et al. The molecular tweezer CLR01 improves behavioral deficits and reduces tau pathology in P301S-tau transgenic mice. Alzheimers Res Ther. 2021;13:6.
78. Bossers K, Wirz KT, Meerhoff GF, Essing AH, van Dongen JW, Houba P, et al. Concerted changes in transcripts in the prefrontal cortex precede neuropathology in Alzheimer's disease. Brain. 2010;133:3699–723.
79. Berchtold NC, Coleman PD, Cribbs DH, Rogers J, Gillen DL, Cotman CW. Synaptic genes are extensively downregulated across multiple brain regions in normal human aging and Alzheimer's disease. Neurobiol Aging. 2013;34:1653–61.
80. Counts SE, Alldred MJ, Che S, Ginsberg SD, Mufson EJ. Synaptic gene dysregulation within hippocampal CA1 pyramidal neurons in mild cognitive impairment. Neuropharmacology. 2014;79:172–9.
81. Saura CA, Deprada A, Capilla-Lopez MD, Parra-Damas A. Revealing cell vulnerability in Alzheimer's disease by single-cell transcriptomics. Semin Cell Dev Biol. 2023;139:73–83.

ACKNOWLEDGEMENTS

We thank Drs. E Sanz and A Quintana for providing the RiboTag mice, A Delprat and VA Díaz for excellent technical support, and M Puigdellívol for critical reading of the manuscript. We thank the Servei d'Estabulari, Servei de Genòmica i Bioinformàtica and Institut de Neurociències Histology and Microscope facilities of UAB, and Genomics Unit of Centre for Genomic Regulation (CRG) for excellent technical support. This work was supported by research projects funded by Agencia Estatal de Investigación, Ministerio de Ciencia, Innovación y Universidades of Spain, with FEDER funds (PID2019-106615RB-I00, PID2022-137668OB-I00 and PDC2021-121350-I00 to CAS; PID2019-107677GB-I00 and PID2022-136597NB-I00 to ARM; SAF2017-89271-R, PID2020-11751ORB-I00 and PID2023-151925OB-I00 to JRA), Junta de Andalucía (P20-0881 to ARM), Instituto de Salud Carlos III (CIBERNED CB06/05/0042 to JRA), and Generalitat de Catalunya (2021 SGR00142) and BrightFocus Foundation (A2022047S to CAS). APD was supported by Juan de la Cierva-Incorporación (IJC2019-042468-I) and Ramón y Cajal (RYC2022-037843-I) Programs, and YAT by a Marie Skłodowska-Curie Postdoctoral Fellowship under the Horizon Europe programme (GA. 101061171). MDCL (BES-2017-082072), PS (PREP2022-000069), AD (FPU 18/02486) and IMG (FPU 17/04283) were supported, respectively, by Formación Personal Investigador and Formación de Profesorado Universitario predoctoral fellowships from Ministerio de Ciencia, Innovación y Universidades of Spain.

AUTHOR CONTRIBUTIONS

MDCL, APD and CAS designed the experiments and coordinated the study. MDCL designed and performed pathological, immunofluorescence and behavioral analyses. MDCL, AD and APD performed the biochemical and expansion microscopy synaptic characterization and transcriptomic analyses. PS performed biochemical analysis. YAT, IMG, HCC and ARM designed and performed the electrophysiological experiments. MDCL, AD, APD, ARM, JRA and CAS discussed and interpreted the data. MDCL, APD and CAS wrote the manuscript with input of all authors. The authors read and approved the final manuscript.

COMPETING INTERESTS

The authors declare no competing interests.

ADDITIONAL INFORMATION

Supplementary information The online version contains supplementary material available at https://doi.org/10.1038/s41380-025-02901-9.

Correspondence and requests for materials should be addressed to Arnaldo Parra-Damas or Carlos A. Saura.